

Mechanism of Hydroxyl Radical-Induced Breakdown of the Herbicide 2,4-Dichlorophenoxyacetic Acid (2,4-D)

Julie Peller, Olaf Wiest,* and Prashant V. Kamat^[a]

Abstract: Oxidative transformations by the hydroxyl radical are significant in advanced oxidation processes for the breakdown of organic pollutants, yet mechanistic details of the reactions are lacking. A combination of experimental and computational methods has been employed in this study to elucidate the reactivity of the hydroxyl radical with the widely used herbicide 2,4-D (2,4-dichlorophenoxyacetic acid). The experimental data on the reactivity of the hydroxyl radical in the degradation of the herbicide 2,4-D were obtained from

γ -radiolysis experiments with both ¹⁸O-labeled and unlabeled water. These were complemented by computational studies of the \cdot OH attack on 2,4-D and 2,4-DCP (2,4-dichlorophenol) in the gas phase and in solution. These studies firmly established the kinetically controlled attack ipso to the ether function-

Keywords: advanced oxidative processes • computer chemistry • herbicide remediation • oxidation • reaction mechanisms

ality as the main reaction pathway of \cdot OH and 2,4-D, followed by homolytic elimination of the ether side chain. In addition, the majority of the early intermediates in the reaction between the hydroxyl radical and 2,4-DCP, the major intermediate, were identified experimentally. While the hydroxyl radical attacks 2,4-D by \cdot OH-addition/elimination on the aromatic ring, the oxidative breakdown of 2,4-DCP occurs through \cdot OH addition followed by either elimination of chlorine or formation of the ensuing dichlorophenoxy radical.

Introduction


The hydroxyl radical, \cdot OH, is the major oxidizing species involved in the advanced oxidation processes of photocatalysis, sonolysis, radiolysis, Fenton-type reactions,^[1] UV-O₃, and UV-H₂O₂ reactions. These processes are linked by the strong oxidative power of the hydroxyl radical. Some of these methods are currently used in environmental remediation processes^[2–4] and others show potential use in the cleanup of contaminated waters and other waste sites.^[5–11] The hydroxyl radical is also generated in living organisms, and its role and effect on the body's chemistry have been under intensive study.^[12] In biological systems, \cdot OH is considered a damaging oxidizer and is believed to be associated with many health problems, diseases, and aging.^[13–15] It is also credited with the

production of other reactive radicals under both normal and stressed physiological conditions. Moreover, radiation therapy creates hydroxyl radicals, which increase the level of cellular damage.^[16–18]

An understanding of the mechanistic details of hydroxyl radical attack on organic compounds is developing slowly and shows variation according to the reaction substrates and conditions. Although a large amount of information concerning the rates of \cdot OH reactions with organic compounds has been compiled,^[19, 20] the details of the reaction mechanisms are incomplete. In order to understand the degradation of environmentally problematic compounds and to determine how damage is caused or prevented in biological processes, the detailed chemistry of the hydroxyl radical with organic compounds must be clarified. The elucidation of the mechanistic pathways is essential for the advancement of these important fields.

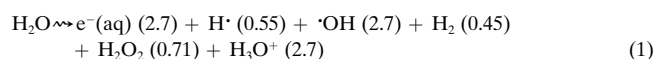
Generation of the powerful hydroxyl radical oxidant for environmental applications can be accomplished by several different means. For example, TiO₂ photocatalysis has been the subject of many investigations.^[21–24] Depending on the source and conditions of its generation, the hydroxyl radical is often accompanied by a variety of other oxidants in the reacting system. These additional oxidants may include hydrogen peroxide (H₂O₂), TiO₂ holes, oxygen, the hydroperoxide radical (HOO \cdot), and the peroxide radical anion

[a] Prof. O. Wiest, Dr. J. Peller, Dr. P. V. Kamat
Radiation Laboratory and Department of Chemistry and Biochemistry
University of Notre Dame, Notre Dame IN 46556-5670 (USA)
Fax: (+1) 574-631-5876
E-mail: owiest@nd.edu

 Supporting information for this article is available on the WWW under <http://www.chemeurj.org> or from the author: Optimized geometries, energies, dipole moments; a scan of energy vs. bond length for the \cdot OH attack at C1 of the ring; a sample HPLC trace, and the GC/MS scans of the labeled water and the 2,4-DCP compounds formed in the labeling experiment.

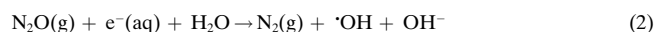
($O_2^{\cdot-}$). Due to the inevitable presence of more than one oxidant in most advanced oxidation systems, the mechanisms of the oxidative transformations involved are quite complex. It then becomes difficult to discern the reactivity of the hydroxyl radical itself. For example, for the TiO_2 /UV light system, Jenks and co-workers identified a lengthy list of intermediates involved in the breakdown of 4-chlorophenol.^[25, 26] Because more than one oxidant is involved in the heterogeneous TiO_2 system, the precise role of the hydroxyl radical is unclear. Radiolytic oxidation, on the other hand, provides an environment in which the number of oxidants can be controlled with the appropriate conditions. Gamma radiolysis thus provides the cleanest experimental system for the study of hydroxyl radical reactivity in aqueous solutions.

If the hydroxyl radical is produced by radiolytic means (γ rays), conditions can be established under which $\cdot OH$ is practically the sole oxidant.^[27] Therefore, in experimental studies of aqueous systems, radiolysis is the most useful method for obtaining information on the extent of the hydroxyl radical reactivity and for determining the products of its reaction with dissolved substances. In the radiolysis of aqueous solutions, $\cdot OH$ is produced by the processes depicted in Equations (1) and (2).^[28]

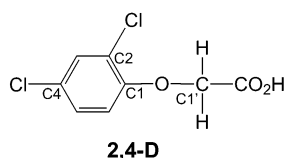


The numbers in parentheses represent the G values, the number of species formed per 100 eV of energy. As long as the concentration of the solute in water is moderate ($< 0.1 M$), the yields of aqueous electrons and hydroxyl radicals are equal.

When an aqueous solution is saturated with nitrous oxide, aqueous electrons are scavenged by the gas to form $N_2O^{\cdot-}$, which immediately decomposes to N_2 and $O^{\cdot-}$. The pK_a of $O^{\cdot-}$ is 11.9; therefore, it is readily protonated by the water to form $\cdot OH$.^[29] The oxygen in this hydroxyl radical originates from the nitrous oxide gas. Half of the hydroxyl radicals from the γ radiolysis of aqueous solutions are produced through the scavenging of the aqueous electron [Eq (2)], the other half are formed from the water solvent [Eq (1)]. Under these experimental conditions, over 90% of the radicals formed in aqueous solutions are the oxidizing $\cdot OH$, while the reducing $\cdot H$ makes up the remainder of the radical population.^[27]



The herbicide 2,4-dichlorophenoxyacetic acid (2,4-D) is a compound of great agricultural, economic, and environmental significance. Starting in 1947, 2,4-D has been used as a herbicide in an effort to enhance agricultural productivity. The use of 2,4-D spread very fast and it ultimately turned into the most utilized herbicide.^[30] In the US alone, it is estimated that 23–30 million kilos of 2,4-D are used annually.^[31] Since the agricultural industry has become dependent upon this compound and its derivatives, concern over its presence in the environment has evolved. Even



though 2,4-D is eventually broken down by microbes in the soil and water with half-lives averaging 3–14 days,^[32] advanced technology is deemed necessary, as the use of this herbicide continues to be great and ubiquitous. The presence of 2,4-D in natural water supplies is a problem that cannot be ignored. Another concern is biological toxification through the formation of stable, toxic intermediates in the herbicide's degradation pathway that can accumulate. In an effort to address these issues, many advanced oxidation processes have been utilized to study and optimize the breakdown of 2,4-D in aqueous solutions.^[33–45]

A major breakdown product identified in studies on the advanced oxidation of 2,4-D in aqueous solutions is 2,4-dichlorophenol (2,4-DCP).^[46] This intermediate is considered to be more toxic than the parent compound, as determined by the microtox bioassay.^[47, 48] Eventually, the oxidative degradation leads to short-chain organic acids, which are much less hazardous substances, before final mineralization to carbon dioxide and water. It is clear that the kinetic data of many organic compounds only relay part of the concerns involved in the remediation processes, since intermediates generated in the breakdown may still be problematic. A complete understanding of the reaction mechanisms and intermediates that take place in the degradation of these compounds is needed to fully address the contamination problems and optimize the oxidation processes.

Here, we report a study on the reactivity of the hydroxyl radical in the degradation of the herbicide 2,4-D. In order to elucidate the mechanism of the hydroxyl radical attack in the degradation of 2,4-D, data from γ -radiolysis experiments with both ^{18}O -labeled water and unlabeled water were analyzed. The experimental work is complemented by computational studies that model the environment in which $\cdot OH$ is the sole or major oxidant in aqueous solutions in order to determine the type and location of the initial reaction between the $\cdot OH$ radical and 2,4-D in the degradative oxidation. This is followed by an analysis of the reactivity of the main intermediate, 2,4-DCP, with the hydroxyl radical in the formation of ensuing intermediates.

Results and Discussion

Reactivity of 2,4-D and the hydroxyl radical: 2,4-D undergoes efficient degradation when subjected to the oxidative conditions of γ radiolysis since it is highly susceptible to attack by the hydroxyl radical.^[37] The intermediates formed in this oxidative breakdown of 2,4-D are 2,4-DCP, 4-chlorocatechol, 2-chlorohydroquinone, hydroxylated 2,4-dichlorophenols, 2,4-dichloroanisole, 1,2,4-trihydroxybenzene, and small amounts of several unidentified compounds. The most prevalent intermediate formed during the early course of the breakdown is 2,4-dichlorophenol, a more toxic compound than 2,4-D. Figure 1 shows the variation in formation of 2,4-dichlorophenol as the concentration of 2,4-D decreases over time when a 0.20 mM aqueous γ solution was subjected to γ radiolysis. Total organic carbon (TOC) analyses, shown in Figure 2, were performed on the aqueous solutions at various times during the radiolysis, and indicate that most of the

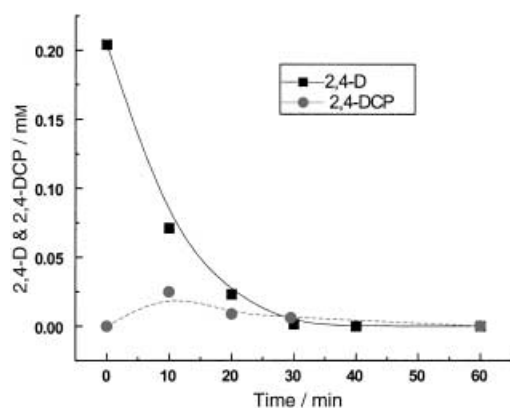


Figure 1. Radiolytic degradation of N_2O saturated aqueous 2,4-D (0.21 mM), and the formation and subsequent degradation of 2,4-DCP.

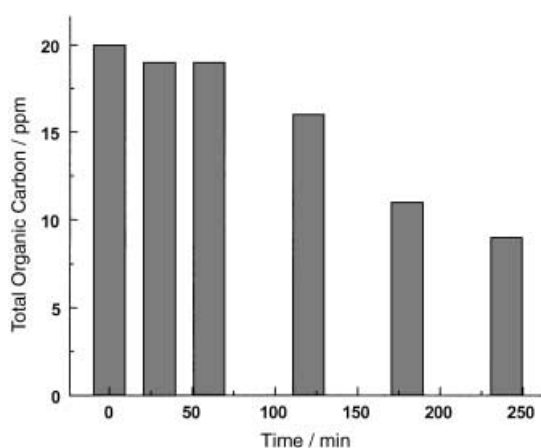


Figure 2. Change in the total organic carbon in the γ radiolysis of 2,4-D (20 ppm carbon) over a 4 hour time period.

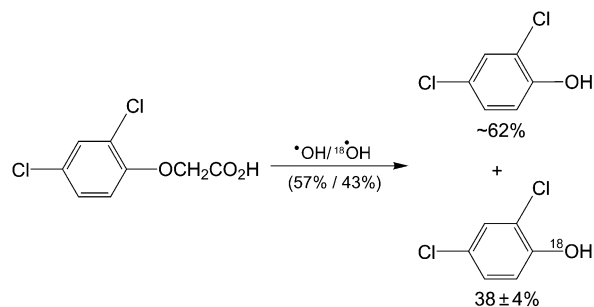
organic carbon remained in solution well after the 2,4-D and 2,4-DCP were completely consumed. This established the presence of other later intermediates formed from the degradation of 2,4-D.

In all experimental oxidative transformations, the single most prevalent intermediate in the reaction between hydroxyl radicals and 2,4-D is 2,4-DCP.^[36–39, 43, 44] As depicted in Figure 1, radiolytic degradation leads to a small build-up of this intermediate. From a mechanistic viewpoint, the formation of this intermediate would indicate a specific site for $\cdot OH$ addition to the 2,4-D ring. For this transformation, an $\cdot OH$ attack at C1 of the aromatic ring, followed by loss of an alkoxy radical or anion to form 2,4-DCP could be envisioned. Alternatively, hydrogen abstraction from the methylene carbon, followed by trapping of the ensuing radical and breaking of the C_1-O bond, in analogy to the mechanism proposed in an earlier study by Li and Jenks, is also possible.^[49] These two pathways differ by which $C-O$ bond, C_1-O or $C_1'-O$, is broken.

In order to obtain more definitive experimental information on the hydroxyl radical attack on the ring, ^{18}O -labeled water was used in the γ radiolysis experiments. A solution of 2,4-D in ^{18}O -labeled water (87% $H_2^{18}O$) was subjected to γ rays, and ^{18}O -labeled, as well as unlabeled ^{16}O , hydroxyl radicals, were generated. Both labeled and unlabeled hydrox-

yl radicals reacted with the herbicide. The experiment was allowed to run for 5 minutes to obtain information about the early stages of the radical pathway. The products were then adsorbed onto a SPME fiber and analyzed by mass spectrometry as described in the Experimental Section.

The mass spectral data revealed the presence of the two expected isotopomers of 2,4-dichlorophenol from the $^{18}OH/\cdot OH$ reactions with 2,4-D (Scheme 1). The labeled 2,4-DCP

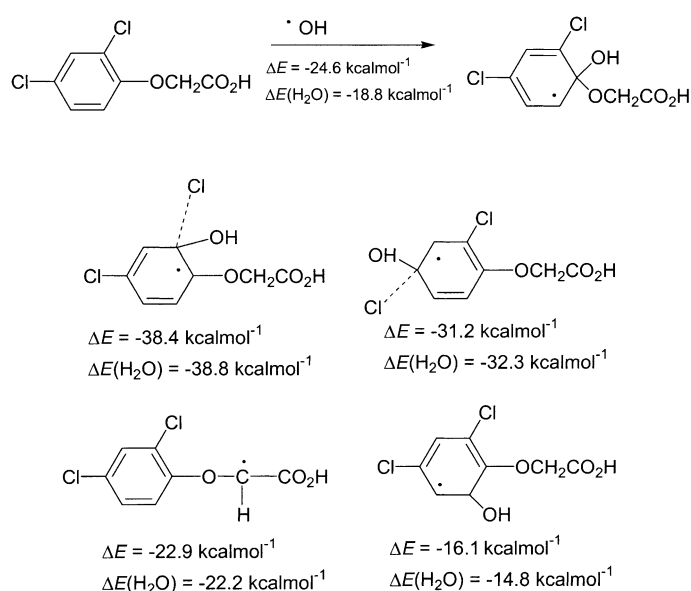


Scheme 1. Initial hydroxyl radical attack on 2,4-D by ^{18}O -labeled and unlabeled hydroxyl radicals. The accuracy of the water analysis is estimated to be $\pm 5\%$.

intermediate was calculated to be present at $38 \pm 4\%$. Once again, the ^{18}O content of the solvent water was 87%, where half of the hydroxyl radicals were formed from the water and half from the nitrous oxide gas. Within experimental accuracy, all the phenolic oxygens of 2,4-DCP originated from hydroxyl radicals. Consequently, the bond between the aromatic carbon and the ether oxygen (C_1-O) is broken in this reaction. The low concentration of 2,4-DCP early in the reaction (see Figure 1) and the slightly higher rate constant of the reaction of the hydroxyl radical with 2,4-D,^[37, 46] make ^{18}O incorporation at the 2,4-DCP stage unlikely. An exchange at the stage of the phenoxy radical can also be excluded since its stationary concentration is low and the reaction is known to lead to different products than the ones observed.^[50] It can therefore be concluded that the formation of 2,4-DCP proceeds by hydroxyl radical addition to the ring in the first step of the mechanism, followed by the loss of the alkoxy group.

While these product studies give strong evidence for a preferred reaction pathway, they do not provide insights into the origin of the observed selectivity. Further analysis of the reaction pathway was therefore pursued by using computational methods. In the initial hydroxyl radical attack on 2,4-D, the energies of the reactants and products were calculated in the gas phase and in a cavity model representing an aqueous solution.

Scheme 2 summarizes the computed results for the reaction energies in the gas phase and in water. The results of these calculations suggest that all addition reactions to the aromatic ring of 2,4-D are energetically favorable. *Ipso* attacks (at carbons 1, 2 and 4 of the aromatic ring) are preferred over attacks at the unsubstituted positions of the ring by a significant margin. This is consistent with the observation that no hydroxylated 2,4-D intermediates were identified in the experimental work.^[37, 46] Attacks at the unsubstituted



Scheme 2. Energies (gas-phase and water-continuum-model) of the radical intermediates formed from various hydroxyl radical attacks on 2,4-D; energies calculated by using B3LYP/6-31G*.

positions are therefore not considered further. The most relevant pathways in the context of the breakdown of 2,4-D are the hydroxyl radical additions at the functionalized positions on the aromatic ring. We will therefore initially focus the discussion of the computational results on the three possible *ipso* attacks.

For the three substituted positions on the 2,4-D molecule, two different types of pathways were found, one for attack at the chlorine-substituted positions C2 and C4, and the other for attack at the oxygen-substituted C1. Reaction of $\cdot\text{OH}$ at C1 leads to the formation of a σ -type adduct that is $24.6 \text{ kcal mol}^{-1}$ lower in energy than the separated species. The length of the newly formed C1–O bond is 1.45 \AA , while that of C1 and the ether oxygen is 1.40 \AA . Scans of both the C–O bond lengths show that $\cdot\text{OH}$ attack at carbon 1 of the ring is barrierless in the gas phase (see Supporting Information).

In contrast, no such σ -type intermediate could be located for the attack of $\cdot\text{OH}$ at either C2 or C4. Instead, the initial product of the approach of a hydroxyl to C2 or C4 of 2,4-D is a π -complex, such as the one shown in Figure 3. The formation of this complex has a reaction energy of $-38.8 \text{ kcal mol}^{-1}$ and is even more exothermic than the formation of the σ -type intermediate discussed above. The carbon–chlorine bond

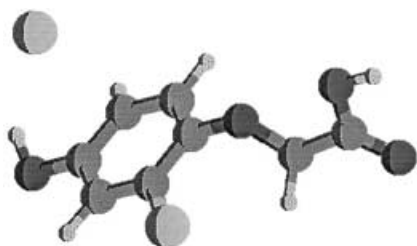


Figure 3. π -Complex formed by $\cdot\text{OH}$ addition at carbon 4 of the aromatic ring.

length is $\sim 2.4 \text{ \AA}$, far from a normal bond length of $\sim 1.7 \text{ \AA}$, and only a weak interaction of the chlorine radical and the aromatic system persists. Due to the rearomatization of the ring, the formation of this π complex from attacks at C2 and C4 is more exothermic by $13.8 \text{ kcal mol}^{-1}$ and $6.6 \text{ kcal mol}^{-1}$, respectively, than the formation of the σ -type adduct. However, none of the products of $\cdot\text{OH}$ attack on C2 or C4 of 2,4-D were detected in this or earlier experimental studies.^[37, 46] Since the energetic preference for the π -type intermediates is significantly larger than the margin of error expected for the computational methodology used, the discrepancy between theory and experiment is not solely explained by the relative stability of the intermediates. We thus studied the pathways leading to the formation of the π complexes in more detail. The results of these calculations are summarized in Figure 4.

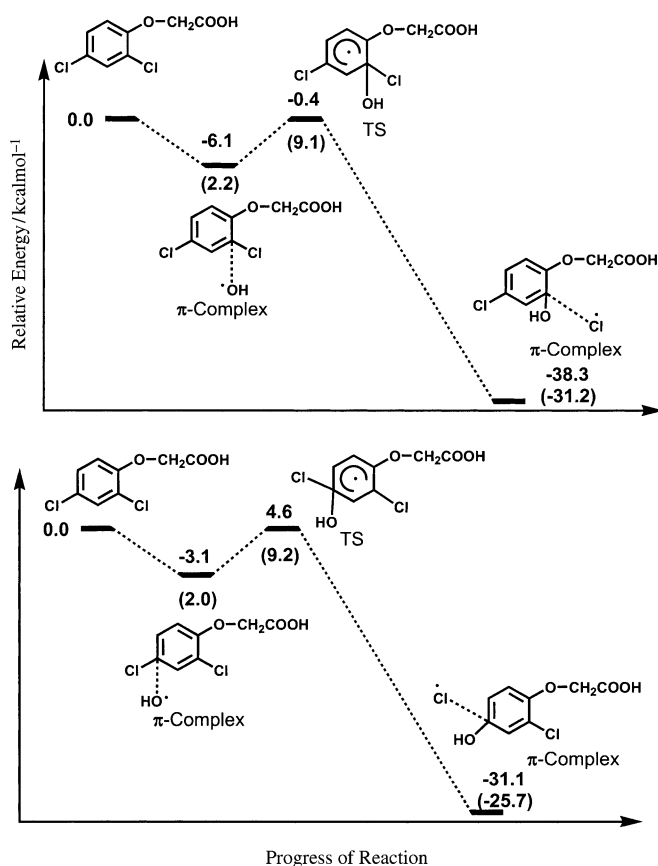


Figure 4. Energy profiles ($\Delta E + \text{ZPE}$ and ΔG) in the $\cdot\text{OH}$ additions on carbon 2 (top) and carbon 4 (bottom) of the aromatic ring (gas-phase values). ΔG values are given in parentheses.

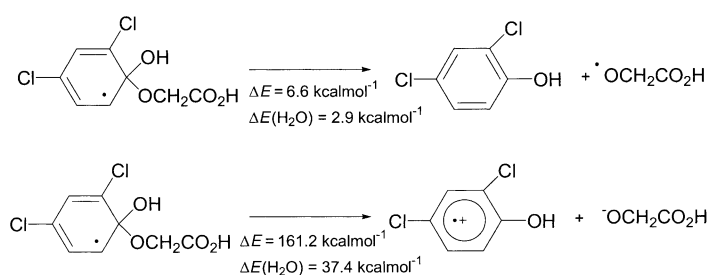
$\cdot\text{OH}$ addition to the aromatic ring at either C2 or C4 begins with the establishment of a π complex in which the forming carbon–oxygen bond is approximately 2.0 \AA . In both cases, the initial complex formation is exothermic, $-6.1 \text{ kcal mol}^{-1}$ for addition at C2 and $-3.1 \text{ kcal mol}^{-1}$ for addition at C4. This complex then proceeds to the transition structure with the input of energy. The activation energies are 5.7 and $7.7 \text{ kcal mol}^{-1}$ at C2 and C4, respectively, from their original π complexes. Thus, a small but significant activation barrier exists in the hydroxyl radical *ipso* attacks at C2 and C4. On the

free-energy surface, these differences are even more pronounced due to the more ordered structure and the resulting loss in entropy. The initial π complex is now $2.2 \text{ kcal mol}^{-1}$ higher in energy than the reactants, while the overall activation energy is $9.1 \text{ kcal mol}^{-1}$. While a direct free energy comparison to the $\cdot\text{OH}$ attack at C1 is difficult because no normal-mode analysis can be performed for this pathway in the absence of a true stationary point, it is clear that there is a true activation barrier on the ΔG surface for the attacks of $\cdot\text{OH}$ at C2 and C4 that is significantly larger than the one for the attack at C1.

From the transition structure, the reaction pathway immediately proceeds energetically downhill in a concerted fashion to form a second π complex, which has the chlorine weakly interacting with the aromatic system. These are the lowest-energy structures depicted in Scheme 2 and Figure 3 from the $\cdot\text{OH}$ *ipso* attacks at C2 and C4. In the $\cdot\text{OH}$ attack at C2, the downhill process from the transition structure is exothermic by $37.9 \text{ kcal mol}^{-1}$. With the attack at C4, the energy release amounts to $31.2 \text{ kcal mol}^{-1}$. Although these calculations do not include solvent effects, it can be expected that the *relative* barriers for the different modes of attack are similar to the gas-phase values.

The thermodynamic data indicate the preferential formation of the products of the $\cdot\text{OH}$ attack at C2 and C4. However, the product of the reaction is determined by the barriers for attack of the hydroxyl radical on the ring: $5.7 \text{ kcal mol}^{-1}$ and $7.7 \text{ kcal mol}^{-1}$, respectively. Similarly, hydrogen abstraction from the side-chain methylene carbon, which had a reaction energy of $-22.9 \text{ kcal mol}^{-1}$ in the gas phase that was thermodynamically competitive with OH attack on C1, has a small but significant activation barrier of $3.5 \text{ kcal mol}^{-1}$. The reaction conditions and the high exothermicity of either reaction do not allow the establishment of an equilibrium. Thus, none of the reaction pathways for which a barrier is predicted by the computations is experimentally observed. In agreement with the calculated barrierless attack at C1, the major observed product is 2,4-DCP. This pathway is also consistent with the results of the labeling studies discussed above. Thus, it is clear that the reaction is kinetically controlled and the barrierless hydroxyl radical attack at C1, leading to the experimentally observed product 2,4-dichlorophenol, is predicted to be dominant pathway.

Details of the $\cdot\text{OH}$ attack at carbon 1 were investigated further by computational analyses. Once the position of the initial attack is established, extrusion of the alkoxy side chain leads to the formation of 2,4-DCP. This bond breakage between the aromatic carbon and the oxygen of the ether can take place in either a heterolytic or homolytic manner. This breakage may be solvent dependent due to the formation of highly solvated ions in the heterolytic cleavage. Therefore, cleavage of the ether group after $\cdot\text{OH}$ addition to the ring was calculated in both gas-phase and water solvent systems. The conductor-like polarizable continuum (CPCM) model simulates the effect of the water solvent^[51] at least in a qualitatively correct manner and has, for example, recently been utilized to calculate pK_a values for organic acids.^[52] Scheme 3 summarizes the results of the calculations. As expected, the homolytic cleavage of the C–O bond is overwhelmingly



Scheme 3. Energies of the homolytic and heterolytic cleavage of the alkoxy group of 2,4-D.

favored over heterolytic break again in the gas phase. However, it is also highly favored in water. Although the cavity model used does not consider specific solvent interactions that could lead to subsequent reactions of either ion formed (such as protonations and deprotonations), the energetic preference of $34.5 \text{ kcal mol}^{-1}$ for the homolytic process is large enough to make this the favored process. Unlike the reaction energies shown in Scheme 2, a large difference is noted between the energies in the heterolytic formation of the 2,4-DCP radical cation and alkoxy anion in water and in the gas phase. Since ions are well stabilized in the water solvent, this large difference was expected. Even so, the stabilization of the ions by water still does not compete well with the more favored homolytic cleavage and formation of the stable 2,4-DCP.

These results suggest that the mechanism of hydroxyl radical attack on 2,4-D begins with $\cdot\text{OH}$ addition to the aromatic ring, followed by loss of the alkoxy group. This mechanism differs from the proposed mechanisms of the $\cdot\text{OH}$ -induced decomposition of anisole by Li and Jenks.^[49] In their study, two competitive pathways, hydrogen abstraction and $\cdot\text{OH}$ addition, were proposed for the hydroxyl-mediated reaction of isotopically labeled anisole with the TiO_2 advanced-oxidation system. In the present study, based on the observed ^{18}O incorporation, we can rule out the hydrogen abstraction pathway. It can thus be concluded that for the $\cdot\text{OH}$ -mediated oxidation of 2,4-D, an addition–elimination pathway dominates. This inconsistency between the two studies is probably due to the different advanced oxidative processes utilized in their experiments (photocatalysis and hydrogen peroxide/UV light) versus the radiolytic system used in our experiments. Gamma radiolysis of N_2O -sparged aqueous solutions generates the hydroxyl radical as the prominent oxidizing species, whereas other advanced oxidative systems involve more than just the hydroxyl radical as the oxidizing species and/or heterogeneous effects at the solid/liquid interface.

The finding that the initial reaction is followed by loss of the alkoxy group leading to 2,4-DCP as the primary product is further supported by previous experimental work, in which the buildup of chloride ions did not occur to any measurable extent in the first few minutes of the radiolysis experiments.^[37] The delayed accumulation of chloride ions suggests that chloride is not lost from the aromatic ring in the initial hydroxyl radical attacks. In fact, the γ -radiolysis experiments revealed a buildup of chloride ions only after the decay of 2,4-

DCP. This observation further supports the fact that 2,4-D transforms to 2,4-DCP before the Cl^- is displaced.

A minor product formed in the γ radiolysis of 2,4-D is 2,4-dichloroanisole. This compound is formed through a minor pathway of decarboxylation, followed by hydrogen abstraction from the solvent. Phenoxyacetic acid compounds are known to undergo decarboxylation reactions under oxidizing conditions.^[53, 54] A very small amount of 2,4-dichloroanisole with no incorporation of labeled oxygen was detected in the ^{18}O water experiments. This further confirms that the decarboxylation pathway that accounts for the presence of this intermediate is a minor side reaction.

Reactivity of 2,4-DCP and the OH radical: The reactivity of the hydroxyl radical with 2,4-dichlorophenol shows several similarities to that with 2,4-D. 2,4-DCP is efficiently degraded in γ -radiolysis experiments; this shows that the hydroxyl radical is comparably effective in attacking the chlorinated phenol. The lifetime of 2,4-DCP upon irradiation with a dose rate of $5.3 \text{ krad min}^{-1}$ is somewhat longer than that of 2,4-D, with a half-life of 13 minutes compared with 9 minutes for 2,4-D. The difference in the calculated lifetimes is explained, at least in part, by the ineffective reaction of the OH radical at carbon 1. Intermediates formed in the hydroxyl-mediated degradation include hydroxylated 2,4-dichlorophenols, 4-chlorocatechol, and 2-chlorohydroquinone. Forty minutes into the radiolysis of 2,4-DCP, only a few aromatic species are still present in very small amounts; this indicates that the reactions between the aromatic intermediates and the hydroxyl radical are also fast. Conversely, the slow loss of organic carbon shows that the smaller nonaromatic compounds have much longer lifetimes in aqueous solution under the radiolytic oxidizing conditions. After 3 hours of γ radiolysis, only about half of the organic carbon was mineralized. Figure 5 shows the change in organic carbon in the γ radiolysis of 2,4-DCP.

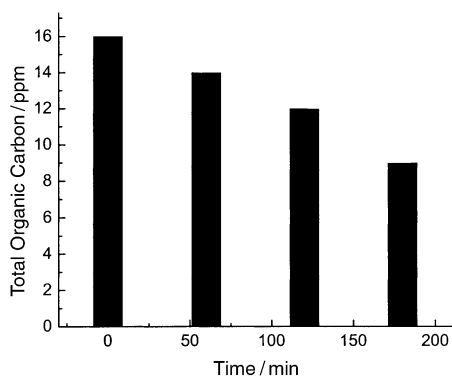
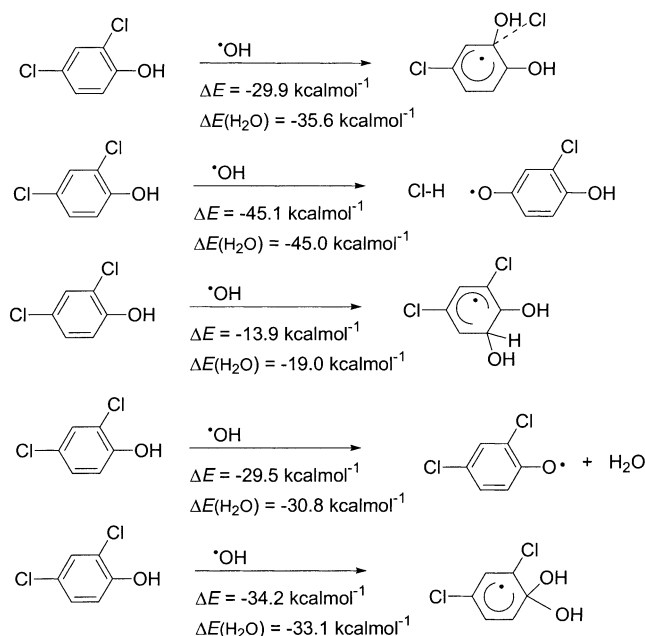


Figure 5. Change in the total organic carbon in the γ radiolysis of N_2O -saturated aqueous 2,4-DCP (16 ppm carbon) over a 3 hour period.

The preferred pathway in the hydroxyl radical reaction with chlorinated phenols is radical addition to the aromatic ring. Many pulse-radiolysis studies on phenol and other benzene derivatives have demonstrated the formation of the cyclohexadienyl radicals upon $\cdot\text{OH}$ addition.^[55–60] Hydroxyl radical additions have also been verified by other experimental work

with substituted phenol compounds.^[61–63] We have investigated the reaction of 2,4-DCP with the hydroxyl radical using computational methods. Our calculations indicate that all the hydroxyl radical additions to the aromatic ring of 2,4-DCP are highly exothermic reactions and are not strongly solvent-dependent. In addition, phenoxy-radical formation through a hydrogen-abstraction reaction is also a favorable reaction. Scheme 4 shows the energies calculated for the various $\cdot\text{OH}$ reactions with 2,4-DCP.



Scheme 4. Gas-phase and water-continuum-model energies of the various hydroxyl radical attacks on 2,4-DCP. Energies calculated by using B3LYP/6-31G*.

Addition of the hydroxyl radical to the substituted carbon atoms is favored over $\cdot\text{OH}$ addition at the unsubstituted position (carbon 6) of the aromatic ring. Formation of the chlorinated phenoxy radical from the $\cdot\text{OH}$ reaction with 2,4-DCP is comparable in energy to the $\cdot\text{OH}$ additions at the substituted positions of the aromatic ring. Since the existence and stability of the phenoxy radical and related species (i.e., tyrosyl radical in biological systems^[64–67]) are well documented, this radical intermediate is considered a viable intermediate in 2,4-DCP oxidation. Experimental $\cdot\text{OH}$ -induced oxidations (γ radiolysis) of 2,4-DCP generate the intermediates 4-chlorocatechol and 2-chlorohydroquinone. Their presence in the oxidation pathway supports the theory of $\cdot\text{OH}$ attack at the carbons bonded to the chlorines on the aromatic ring, exemplified in the first two reactions of Scheme 4.

The calculated structures of the reaction intermediates from the $\cdot\text{OH}$ additions vary according to position of attack. For $\cdot\text{OH}$ attack at carbon 4, the optimized geometry consists of two separated species, the phenoxy radical and hydrogen chloride, while the $\cdot\text{OH}$ attack at carbon 2 proceeds via a π complex. These reaction intermediates are different from those formed from $\cdot\text{OH}$ addition at carbons 1 and 6. Moreover, the high exothermicity of the $\cdot\text{OH}$ addition at carbon 4 ($-45.1 \text{ kcal mol}^{-1}$) is partly due to the re-establishment of

aromaticity. The other reaction that leads to an optimized intermediate with aromatic character is the hydrogen abstraction reaction, which forms the chlorinated phenoxy radical.

A comparison of reaction energies can be made between the intermediates formed from the $\cdot\text{OH}$ attacks at carbons 1 and 6. The hydroxyl radical adds to the ring at both of these positions to form optimized σ complexes. The calculated energies for these reactions are substantially different. For attack at carbon 1, 34.2 kcal mol⁻¹ of energy is released, while attack at carbon 6 is exothermic by only 13.9 kcal mol⁻¹. Once again, these computational results indicate that $\cdot\text{OH}$ addition at the unsubstituted positions of the ring is not likely.

All three hydroxylated isomers of 2,4-DCP have been detected experimentally in the $\cdot\text{OH}$ -mediated oxidation of 2,4-DCP. Since $\cdot\text{OH}$ attack at the unsubstituted positions of the ring is energetically less favored than the alternative reactions (Scheme 4), a pathway that involves a phenoxy radical intermediate is postulated in the formation of these compounds. According to our calculations, the energy of reaction of 2,4-DCP with the hydroxyl radical to form the chlorinated phenoxy radical is -29.4 kcal mol⁻¹, as shown in Scheme 4. Also, the phenoxy radical may be formed after an $\cdot\text{OH}$ addition to the ring, for example at carbon 4, which is followed by loss of HCl.

ESR studies and other theoretical studies have shown that the radical character of phenoxy radicals is well dispersed in the aromatic ring, giving relatively high stability to the radical.^[68–71] The spin densities obtained from our calculations confirm this radical dispersion. Figure 6 shows the spin-density values for the 2,4-dichlorophenoxy radical. The carbons bear a large part of the radical character; this indicates that further radical reactions are possible on the ring.

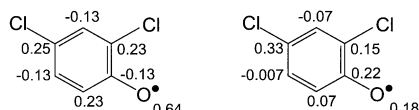
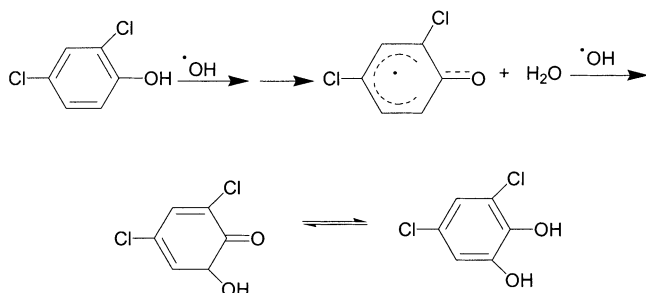


Figure 6. Spin densities of the 2,4-dichlorophenoxy radical, calculated in both the gas phase (left) and in a water solvent continuum (right).

The postulated $\cdot\text{OH}$ reaction pathway for the formation of hydroxylated dichlorophenols, is shown in Scheme 5. The phenoxy radical is formed first. After an $\cdot\text{OH}$ attack on an unsubstituted position of the phenoxy radical, the compound



Scheme 5. Proposed reaction pathway in the formation of the dihydroxylated 2,4-DCP molecule

tautomerizes to the lower-energy aromatic system. The overall scheme requires two $\cdot\text{OH}$ and is highly exothermic with an overall reaction energy of -101.3 kcal.

An alternative pathway to the formation of the hydroxylated 2,4-DCP isomers is direct $\cdot\text{OH}$ addition to 2,4-DCP. Direct additions to unsubstituted positions of the ring will lead to the hydroxylated 2,4-DCP isomers. (Scheme 4, reaction 3) These transformations require the loss of a hydrogen atom (a highly reactive reducing species) after the hydroxyl radical addition. The computational analysis of this pathway indicates a slightly endothermic process overall (4.8 kcal mol⁻¹). This pathway is therefore not competitive with the highly exothermic reactions discussed above.

Conclusion

Mechanistic information on the reactivity of the hydroxyl radical with the herbicide 2,4-D has been obtained by using a combination of experimental and computational investigations. The major pathway begins with $\cdot\text{OH}$ addition to the aromatic ring of 2,4-D, which is followed by the loss of the alkoxy radical to form 2,4-DCP, the prominent intermediate in the degradation. The $\cdot\text{OH}$ -mediated transformations of 2,4-DCP are similar in reactivity to those of 2,4-D, but probably also include the chlorinated phenoxy radical in the formation of some of the intermediates. As the reaction proceeds beyond the early intermediates of the 2,4-DCP oxidation, more polar and ionic non-aromatic species form. Detection of these types of compounds requires the use of different analytical tools than those used for the early stages of the mechanism. The experimental work to investigate the further fate of these species is currently in progress.

Experimental Section

Chemicals: 2,4-dichlorophenoxyacetic acid (Aldrich, 99%), 2,4-dichlorophenol (Aldrich, 99%), catechol (Aldrich, 99%), chlorohydroquinone (Aldrich, 85%), 4-chlorocatechol (TCI, 99%), hydroquinone (Aldrich, 99%), 4,6-dichlororesorcinol (Aldrich, 97%), 2,4-dichloroanisole (Lancaster, 99%), 2,4-D methyl ester (Chem Service, 99.5%), ¹⁸O-labeled water (Isotec, minimum 95 atom % ¹⁸O; Medical Isotopes, Inc. 95.1% H₂¹⁸O) were used as supplied. Unbuffered aqueous solutions were prepared by using Milli-Q purified water. High-purity N₂O gas was supplied by Mittler Supply Co., South Bend, IN and further filtered through a drying agent.

γ -Radiolysis experiments: γ -radiolysis experiments were conducted with a Shepherd 109 ⁶⁰Co source. The aqueous solutions were sparged with N₂O(g) for 45 min in glass vials, which were capped with a rubber septum before γ irradiation. Samples were taken at the indicated times. Fricke dosimetry was performed to determine the dose rate. A dose rate of 5.3 krad min⁻¹ was determined by using a H₂SO₄/FeNH₄SO₄ (0.40:10.0 mM) dosimetry solution.

Isolation of intermediates by using SPME methods for GC/MS analysis: Solid-phase microextraction (SPME) fibers were obtained from Supelco Chromatography. Two different fiber types were utilized, 65 μ m and 70 μ m carbowax/divinylbenzene on a StableFlex fiber. For each trial run, the fiber was submerged in the aqueous solution for 1 h with stirring. It was then immediately placed into the GC/MS injector, where it was allowed to desorb for 10 min at 230 °C. GC/MS data were acquired on a Varian Saturn 2000 GC/MS system equipped with a Varian Star 3400 CX gas chromatograph. The GC column was a J&W#38;W Scientific DB-5 column

measuring 30 m × 0.250 mm, with a 0.25 μm film thickness. The temperature program began at 50 °C, at which it was maintained for 10 min for complete desorption of the organics on the fiber. The column oven temperature was then increased by 10 °C min⁻¹ to 250 °C and then held constant.

Identification of intermediates: Intermediates were identified by comparison with authentic samples by using a Waters HPLC system (Millennium32 2010, Waters 717 plus Autosampler, Waters 600 Controller Solvent Pump) with an Alltech Econosphere C8 column: 5 μm; 250 × 4.6 mm. A solvent gradient was utilized that consisted of methanol, water, and 1% aqueous acetic acid for 30 minutes at 1.2 mL min⁻¹. The solvent mixture started as 6% methanol, 92% water and 2% of the acetic acid solution. By 18 minutes, the mixture was 70% methanol, 27% water and 3% acetic acid solution, then it was returned to the original composition by the 30 minute mark. The intermediates were monitored at 285 nm with a photo diode array detector and were also identified by using the Varian GC/MS system described earlier.

Total organic carbon analyses: Mineralized carbon was measured by using a Shimadzu total organic carbon (TOC) analyzer, model TOC-5050 equipped with an ASI-500A autosampler. All analyses were performed in triplicate.

Experiments with H₂¹⁸O: ¹⁸O water was purchased from Isotec and from Medical Isotopes, Inc. and contained 95.4 and 95.1 atom% ¹⁸O, respectively, according to the specification sheets. We analyzed all of the H₂¹⁸O samples by GC/MS and determined the labeled-compound enrichment (H₂¹⁸O) to be 87 and 88% for the Isotec samples and 87% for the Medical Isotope samples (see Supporting Information). 5.0 mL of a solution of 2,4-D in methanol (0.5 mm) were transferred to a round-bottom flask and evaporated to dryness. The flask was then set on a vacuum line for 3 hours. Approximately 1 mL of ¹⁸O-labeled water was transferred by syringe from the original vial to the flask. It was stirred for several minutes and transferred to a small sealed vial. Nitrous oxide was bubbled into the vial for several minutes, and then the solution was subjected to γ rays for 5 minutes. Reaction products were adsorbed onto the SPME fiber and analyzed by GC/MS. The isolation and analysis of intermediates was repeated with the SPME fiber and GC/MS five times. The ¹⁸O water was also checked after the γ radiolysis experiments and the isotopic concentration remained at 87%; this indicated that no significant contamination by moisture had taken place.

GC/MS studies of labeled compounds: GC/MS experiments were performed on a JEOL GC Mate equipped with an HP6890 GC and autosampler. The GC was operated under the following conditions: column, HP-5 30 m × 0.32 mm i.d., 0.25 μm film thickness; injector temperature, 180 °C; column program, 50 °C for 1 min ramp to 250 °C at 10 °C min⁻¹. EI mass spectra were acquired by using magnet scans over the mass range 10–50 at a rate of 0.8 s per scan.

Analysis of the 2,4-dichlorophenol MS data: The isotopic pattern, due to the presence of two chlorines on the ring, should show mass spectrum peaks for the 2,4-DCP compound at 162, 164, and 166 in a 9:6:1 ratio. The compound was tested several times on the GC/MS, and the response of the instrument to the peak at 164 in comparison to the peak at 162 was 72% ± 2%, instead of the expected 67%. When this response was combined with the data from the labeled water experiments, the percentage of the labeled 2,4-dichlorophenol was determined to be 38% ± 4 (see Supporting Information).

Computational studies: All geometries were optimized at the B3LYP/6-31G* level of theory by using the Gaussian 98 series of programs.^[73] This level of theory has been shown to adequately predict reaction energies and transition-state energies for radical pathways.^[74–76] In particular, Hadad and co-workers demonstrated that for additions of ·OH to aromatic hydrocarbons, the activation energies calculated by B3LYP/6-31G* matched well with the experimental data.^[74] B3LYP/6-31 + G* single-point calculations demonstrated that this basis set is converged (see Supporting Information). All energies are corrected for zero-point energies from harmonic-frequency analysis of the B3LYP/6-31G* optimized structures. Solvent effects were evaluated by using the CPCM model for water and the default values for the cavity with $\alpha = 1.4$ and 60 tesserae. Energies from the CPCM calculations were corrected for zero-point energies by using the results of the gas-phase calculations.

Acknowledgements

We extend special thanks to Bill Boggess in the Mass Spectrometry Facility at the University of Notre Dame for his help in the analysis of the various labeled compounds, to Ian Duncanson for construction of the glass apparatus used in the labeling experiments, to K. Vinodgopal, Indiana University Northwest, for assistance with the SPME experiments, and to the IUN Chemistry Department for the use of their facilities. The work described herein was supported by the Office of Basic Energy Sciences of the US Department of Energy. This is contribution no. NDRL 4351 from Notre Dame Radiation Laboratory.

- [1] B. Ensuing, F. Buda, P. Blochl, E. J. Baerends, *Angew. Chem.* **2001**, *113*, 2977; *Angew. Chem. Int. Ed.* **2001**, *40*, 2893.
- [2] N. Getoff in *Environmental Applications of Ionizing Radiation* (Eds.: W. J. Cooper, R. D. Curry, K. E. O'Shea), Wiley, New York, **1998**, p. 231.
- [3] M. G. Nickelson, D. C. Kajdi, W. J. Cooper, C. N. Kurucz, T. D. Waite, F. Gensel, H. Lorenzl, U. Sparka in *Environmental Applications of Ionizing Radiation* (Eds.: W. J. Cooper, R. D. Curry, K. E. O'Shea), Wiley, New York, **1998**, p. 451.
- [4] F. Taghipou, G. Evans in *Environmental Applications of Ionizing Radiation* (Eds.: W. J. Cooper, R. D. Curry, K. E. O'Shea), Wiley, New York, **1998**, p. 477.
- [5] H. Destaillets, T. Lesko, M. Knowlton, H. Wallace, M. R. Hoffman, *Ind. Eng. Chem. Res.* **2001**, *40*, 3855.
- [6] H. Al-Ekabi, A. Safarzadeh-Amir, W. Sifton, J. Story, *Int. J. Environ. Pollut.* **1991**, *1*, 125.
- [7] F. J. Rivas, F. J. Beltran, O. Gimeno, J. Frades, *J. Agric. Food Chem.* **2001**, *49*, 1873.
- [8] G. Li Puma, P. L. Yue, *Ind. Eng. Chem. Res.* **2001**, *40*, 5162.
- [9] L. H. Thompson, L. K. Doraiswamy, *Ind. Eng. Chem. Res.* **1999**, *38*, 1215.
- [10] S.-A. Lee, K.-H. Choo, C.-H. Lee, H.-I. Lee, T. Hyeon, W. Choi, H.-H. Kwon, *Ind. Eng. Chem. Res.* **2001**, *40*, 1712.
- [11] S. S. Gupta, M. Stadler, C. A. Noser, N. Ghosh, B. Steinhoff, D. Lenoir, C. Horwitz, K.-W. Schramm, T. J. Collins, *Science* **2002**, *296*, 326.
- [12] B. N. Ames, M. K. Shigenaga, T. M. Hagen, *Biol. Oxid. Antioxid.* **1994**, *90*, 193.
- [13] Z. Shen, W. Wu, S. L. Hazen, *Biochemistry* **2000**, *39*, 5474.
- [14] B. Halliwell in *Free Radical in Biology* (Eds.: B. Halliwell, J. C. Gutteridge), Clarendon Press, New York, **1989**.
- [15] C. von Sonntag, *The Chemical Basis of Radiation Biology*, Taylor & Francis, London, **1987**.
- [16] M. D. Sevilla, D. Becker in *Advances in Radiation Biology, Vol. 17* (Ed.: J. Lett), Academic Press, New York, **1993**, p. 121.
- [17] M. Mori, S.-I. Teshima, H. Yoshimoto, S.-I. Fujita, R. Taniguchi, H. Hattai, S.-I. Nishimoto, *J. Phys. Chem. B* **2001**, *105*, 2070.
- [18] W. Adam, S. Marquardt, C. R. Saha-Moller, *Photochem. Photobiol.* **1999**, *70*, 287.
- [19] G. Buxton, C. Greenstock, W. P. Helman, A. B. Ross, *J. Phys. Chem. Ref. Data* **1988**, *17*, 513.
- [20] S. Gordon, J. C. Sullivan, A. B. Ross, *J. Phys. Chem. Ref. Data* **1986**, *15*, 1357.
- [21] D. F. Ollis, H. Al-Ekabi, *Photocatalytic Purification and Treatment of Water and Air, Vol. 3*, Elsevier, Amsterdam, **1993**.
- [22] D. F. Ollis, N. Serpone, E. Pelizzetti in *Photocatalysis. Fundamentals and Applications* (Eds.: N. Serpone, E. Pelizzetti), Wiley, New York, **1989**, p. 603.
- [23] C. S. Turchi, D. F. Ollis, *J. Phys. Chem.* **1988**, *92*, 6852.
- [24] C. S. Turchi, D. F. Ollis, *J. Catal.* **1990**, *122*, 178.
- [25] X. J. Li, J. W. Cubbage, T. A. Tetzlaff, W. S. Jenks, *J. Org. Chem.* **1999**, *64*, 8509.
- [26] X. J. Li, J. W. Cubbage, W. S. Jenks, *J. Org. Chem.* **1999**, *64*, 8525.
- [27] R. V. Bensasson, E. J. Land, T. G. Truscott, *Flash Photolysis and Pulse Radiolysis: Contributions to the Chemistry of Biology and Medicine*, Pergamon, New York, **1983**.
- [28] A. J. Swallow, *Radiation Chemistry*, Wiley, New York, **1973**.
- [29] G. V. Buxton, *Trans. Faraday Soc.* **1970**, *66*, 1656.

- [30] I. C. Munro, G. L. Carlo, J. C. Orr, K. G. Sund, R. M. Wilson, E. Kennepohl, B. S. Lynch, M. Jablinski, N. L. Lee, *J. Am. Coll. Toxicol.* **1992**, 2.
- [31] S. O. Archibald, C. K. Winter in *Chemicals in the Human Food Chain*, Van Nostrand–Reinhold, NY, **1990**, p. 1.
- [32] R. G. Wilson, H. H. Cheng, *Weed Sci.* **1976**, 24, 461.
- [33] J. M. Herrmann, J. Disdier, P. Pichat, S. Malato, J. Blanco, *Appl. Catal. B* **1998**, 17, 15.
- [34] K. Djebbar, T. Sehili, *Pest. Sci.* **1998**, 54, 269.
- [35] A. D. Modestov, O. Lev, *J. Photochem. Photobiol. A* **1998**, 112, 261.
- [36] T. S. Muller, Z. L. Sun, G. Kumar, K. Itoh, M. Murabayashi, *Chemosphere* **1998**, 36, 2043.
- [37] J. Peller, MS thesis, University of Notre Dame (USA), **1999**.
- [38] P. Pichat, J.-C. D'Oliveira, J.-F. Maffre, D. Mas in *Photocatalytic Purification and Treatment of Water and Air* (Ed.: D. F. Ollis, H. Al-Ekabi), Elsevier, Amsterdam, **1993**.
- [39] J. J. Pignatello, *Environ. Sci. Technol.* **1992**, 26, 944.
- [40] J. Prado, J. Arantegui, E. Chamarro, S. Esplugas, *Ozone Sci. Eng.* **1994**, 16, 235.
- [41] L. Sanchez, J. Peral, X. Domenech, *Electrochim. Acta* **1996**, 41, 1981.
- [42] a) Y. Sun, J. J. Pignatello, *Environ. Sci. Technol.* **1993**, 27, 304; b) Y. Sun, J. J. Pignatello, *J. Agric. Food Chem.* **1993**, 41, 1139. c) Y. Sun, J. J. Pignatello, *Environ. Sci. Technol.* **1995**, 29, 2065.
- [43] R. Zona, S. Solar, K. Sehested, J. Holcman, S. P. Mezyk, *J. Phys. Chem. A* **2002**, 106, 6743.
- [44] M. Trojanowicz, P. Drzewicz, P. Panta, W. Gluszewski, G. Nalecz-Jawecki, J. Sawicki, M. H. O. Sampa, H. Oikawa, S. I. Borrelly, M. Czaplicka, M. Szewczynska, *Rad. Phys. Chem.* **2002**, 65, 357.
- [45] M. Trillas, J. Peral, X. Domenech, *Appl. Catal. B* **1995**, 5, 377.
- [46] a) J. Peller, O. Wiest, P. V. Kamat, *J. Phys. Chem. A* **2001**, 105, 3176; b) J. Peller, O. Wiest, P. V. Kamat, *Environ. Sci. Technol.* **2003**, 37, 1926.
- [47] M.-C. Lu, J.-N. Chen, *Water Sci. Technol.* **1997**, 36, 117.
- [48] Y. Beaton, L. J. Shaw, L. A. Glover, A. A. Meharg, K. Killham, *Environ. Sci. Technol.* **1999**, 33, 4086.
- [49] X. Li, W. S. Jenks, *J. Am. Chem. Soc.* **2000**, 122, 11 864.
- [50] S. Gopalan, P. E. Savage, *J. Phys. Chem.* **1994**, 98, 12 646.
- [51] V. Barone, M. Cossi, *J. Phys. Chem. A* **1998**, 102, 1995.
- [52] M. D. Liptak, G. C. Shields, *J. Am. Chem. Soc.* **2001**, 123, 7314.
- [53] C. S. Rajesh, T. L. D. S. Thanulingam, *Tetrahedron* **1997**, 53, 16 817.
- [54] N. Somasundaram, C. Srinivasan, *J. Photochem. Photobiol. A* **1996**, 99, 67.
- [55] M. Roder, L. Wojnarovits, G. Foldiak, S. S. Emmi, G. Beggiato, M. D'Angelantonio, *Radiat. Phys. Chem.* **1999**, 54, 475.
- [56] E. Bjergbakke, A. Sillesen, P. Pagsberg, *J. Phys. Chem.* **1996**, 100, 5729.
- [57] G. E. Adams, J. W. Boag, J. Carrant, M. B. Michael in *Pulse Radiolysis* (Eds.: M. Ebert, J. P. Keene, A. J. Swallow, J. H. Baxendale), Academic Press, New York, **1965**, p. 131.
- [58] X.-M. Pan, M. N. Schuchmann, C. von Sonntag, *J. Chem. Soc. Perkin Trans. 2* **1993**, 2, 289.
- [59] A. Wahner, C. Zetzsch, *J. Phys. Chem.* **1983**, 87, 4945.
- [60] E. J. Land, M. Ebert, *Trans. Faraday Soc.* **1967**, 63, 1181.
- [61] U. Stafford, K. Gray, P. V. Kamat, *J. Phys. Chem.* **1994**, 98, 6343.
- [62] S. Solar, *Radiat. Phys. Chem.* **1985**, 26, 103.
- [63] K. I. Priyadarsini, T. P. A. Devasagayam, M. N. A. Rao, S. N. Guha, *Radiat. Phys. Chem.* **1999**, 54, 551.
- [64] C. D. Borman, C. G. Sells, C. Wright, A. G. Sykes, *Pure Appl. Chem.* **1998**, 70, 897.
- [65] A. Ivancich, P. Dorlet, D. B. Goodin, S. Un, *J. Am. Chem. Soc.* **2001**, 123, 5050.
- [66] P. Dorlet, A. W. Rutherford, S. Un, *Biochemistry* **2000**, 39, 7826.
- [67] F. Dole, B. A. Ciner, C. W. Hoganson, G. T. Babcock, R. D. Britt, *J. Am. Chem. Soc.* **1997**, 119, 11 540.
- [68] P. Neta, R. W. Fessenden, *J. Phys. Chem.* **1974**, 78, 523.
- [69] D. Chipman, R. Liu, X. Zhou, P. Pulay, *J. Phys. Chem.* **1994**, 100, 5023.
- [70] G. N. R. Tripathi, *J. Phys. Chem. A* **1998**, 102, 2388.
- [71] B. C. Gilbert, P. Hanson, W. J. Ishham, A. C. Whitwood, *J. Chem. Soc. Perkin Trans. 2* **1988**, 12, 2077.
- [72] M. J. Lundqvist, L. A. Eriksson, *J. Phys. Chem. B* **2000**, 104, 848.
- [73] Gaussian 98 (Revision A.9), M. J. Frisch, G. W. Trucks, H. B. Schlegel, G. E. Scuseria, M. A. Robb, J. R. Cheeseman, V. G. Zakrzewski, J. A. Montgomery, Jr., R. E. Stratmann, J. C. Burant, S. Dapprich, J. M. Millam, A. D. Daniels, K. N. Kudin, M. C. Strain, O. Farkas, J. Tomasi, V. Barone, M. Cossi, R. Cammi, B. Mennucci, C. Pomelli, C. Adamo, S. Clifford, J. Ochterski, G. A. Petersson, P. Y. Ayala, Q. Cui, K. Morokuma, D. K. Malick, A. D. Rabuck, K. Raghavachari, J. B. Foresman, J. Cioslowski, J. V. Ortiz, A. G. Baboul, B. B. Stefanov, G. Liu, A. Liashenko, P. Piskorz, I. Komaromi, R. Gomperts, R. L. Martin, D. J. Fox, T. Keith, M. A. Al-Laham, C. Y. Peng, A. Nanayakkara, M. Challacombe, P. M. W. Gill, B. Johnson, W. Chen, M. W. Wong, J. L. Andres, C. Gonzalez, M. Head-Gordon, E. S. Replogle, J. A. Pople, Gaussian, Inc., Pittsburgh, PA, **1998**.
- [74] C. Barckholtz, T. Barckholtz, C. M. Hadad, *J. Phys. Chem. A* **2001**, 105, 140.
- [75] a) T. S. Dibble, *J. Am. Chem. Soc.* **2001**, 123, 4228; b) J. R. B. Gomes, M. A. V. Ribeiro da Silva, *J. Phys. Chem. A* **2003**, 107, 869.
- [76] J. Korchowiec, *J. Phys. Org. Chem.* **2002**, 15, 524.

Received: October 1, 2002
Revised: June 26, 2003 [F4469]